Available online at www.sciencedirect.com

SCIENCE DIRECT®

Journal of Applied Geophysics 56 (2004) 281–294

JOURNAL OF APPLIED GEOPHYSICS

www.elsevier.com/locate/jappgeo

The relationship of total dissolved solids measurements to bulk electrical conductivity in an aquifer contaminated with hydrocarbon

Eliot A. Atekwana[a], Estella A. Atekwana[a,*], Rebecca S. Rowe[b], D. Dale Werkema Jr.[c], Franklyn D. Legall[d]

[a]*Department of Geological Sciences and Engineering, University of Missouri-Rolla 1870 Miner Circle, Rolla, MO 65409, United States*
[b]*Department of Geology, Indiana University Purdue University Indianapolis 723 W. Michigan Ave, Indianapolis, IN 46202, United States*
[c]*U.S. Environmental Protection Agency, National Exposure Research Laboratory, Environmental Sciences Division, Characterization and Monitoring Branch, Las Vegas, NV, United States*
[d]*The Gillette Company, Environmental Affairs, 37 A Street, Needham, MA 02492-9120, United States*

Received 14 April 2003; accepted 6 August 2004

Abstract

A recent conceptual model links higher bulk conductivities at hydrocarbon impacted sites to higher total dissolved solids (TDS) resulting from enhanced mineral weathering due to acids produced during biodegradation. In this study, we evaluated the above model by investigating the vertical distribution of bulk conductivity, TDS, and specific conductance in groundwater. The results showed higher TDS at contaminated locations consistent with the above model. Further, steep vertical gradients in bulk conductivity and TDS suggest vertical and spatial heterogeneity at the site. We observed that at fluid conductivities <40 mS/m, bulk conductivity was inversely related to fluid conductivity, but at fluid conductivities >40 mS/m, bulk conductivity increased with increasing fluid conductivity. However, at fluid conductivities >80 mS/m, bulk conductivities increased without a corresponding increase in fluid conductivity, resulting in a poor correlation between bulk conductivity and fluid conductivity for the contaminated samples. This suggests that electrolytic conductivity was not completely responsible for the observed variability in bulk conductivity. We suggest two possible reasons for the inverse relationship at low fluid conductivity and poor positive correlation at high fluid conductivity: (1) geochemical heterogeneity due to biological processes not captured at a scale comparable to the bulk conductivity measurement and (2) variability in the surface conductivity, consistent with a simple petrophysical model that suggests higher surface conductivity for contaminated sediments. We conclude that biodegradation processes can impact both electrolytic and surface conduction properties of contaminated sediments and these two factors can account for the higher bulk conductivities observed in sediments impacted by hydrocarbon.
Published by Elsevier B.V.

Keywords: Biodegradation; Bulk conductivity; Contamination; Hydrocarbon; Total dissolved solids

* Corresponding author. Tel.: +1 573 341 6104; fax: +1 573 341 6935.
E-mail address: atekwana@umr.edu (E.A. Atekwana).

0926-9851/$ - see front matter. Published by Elsevier B.V.
doi:10.1016/j.jappgeo.2004.08.003

1. Introduction

Petroleum hydrocarbons remain one of the most prevalent groups of soil contaminants. Consequently, a variety of geophysical techniques have been used to detect their presence and distribution in the subsurface. We believe that the use of geophysical techniques (specifically geoelectrical) at hydrocarbon contaminated sites will become increasingly important not only in providing characterization of the subsurface geology and contaminant distribution, but also in understanding the impacts of biogeochemical processes on the electrical properties of the sediments. Therefore, understanding the relationship between the geoelectrical properties of hydrocarbon-impacted sediments and ongoing physical and biogeochemical processes is a key to the successful application of geoelectrical methods as proxies of these processes.

Until recently, it has commonly been assumed that hydrocarbon-impacted sediments can be effectively imaged only by their higher resistivities compared to "background" due to the partial replacement of conductive soil and pore water by highly resistive petroleum compounds (e.g., Mazác et al., 1990; Schneider and Greenhouse, 1992; De Ryck et al., 1993). This premise is correct as long as the hydrocarbon is fresh, or has not been physically, chemically, or biologically altered. There is ample evidence in the geochemical and microbiological literature to suggest physical and chemical alteration of hydrocarbons in contaminated sediments by indigenous microorganisms (e.g., Cozzarelli et al., 1990, 1994, 2001). Because of the partitioning of hydrocarbons into different phases (free, dissolved, and residual) in the subsurface and the time-dependent biological transformation of hydrocarbons, the chemical and physical properties of hydrocarbon-contaminated sediments are expected to vary with time and in space at contaminated sites.

Geoelectrical investigations at aged (i.e. altered) hydrocarbon spill sites have documented higher bulk conductivities coincident with the zones of hydrocarbon impact (Sauck et al., 1998; Atekwana et al., 2000, 2002, 2004; Shevnin et al., 2003; Abdel Aal et al., 2003; Werkema et al., 2003). Sauck (2000) has proposed a model attributing the higher bulk conductivity to biodegradation. Central to this conceptual conductive layer model is the increase in the total dissolved solids (TDS) in groundwater due to enhanced weathering of minerals from acids produced as byproducts of the degradation process. Thus, TDS is a likely geochemical parameter that closely links the bulk conductivity to microbial degradation of hydrocarbon.

TDS of natural waters can be measured by standard gravimetric techniques or by the use of conductivity/TDS meters. The specific conductance (electrical conductivity normalized to 25 °C) of groundwater is directly related to the TDS based on the assumption that TDS in the water consist mainly of ionic constituents that conduct electricity (e.g., Wood, 1976; Hem, 1985; Lloyd and Heathcote, 1985). In groundwater contaminated with hydrocarbon, it is not clear if the TDS calculated from specific conductance measurements is entirely due to ionic species. There is always a possibility that for groundwater contaminated with dissolved hydrocarbons there may be a reduction of the specific conductance due to the higher resistivity of the hydrocarbon components. Also, it is possible that there could be an enhancement of the specific conductance of groundwater from polar organic compounds (e.g., organic acids and biosurfactants) produced during degradation (Cassidy et al., 2001). In groundwater undergoing natural chemical evolution, TDS measured by the gravimetric method and conductivity/TDS meter is expected to be the same. Thus, consistency between the two methods can be used to validate the TDS calculated from specific conductance routinely measured for groundwater in field settings. For the above reasons, this paper evaluates TDS data from both methods.

This study was conducted as part of a larger research effort to investigate the effect of biogeochemical processes on the geoelectrical properties of hydrocarbon-contaminated sites. In this study, we measured the vertical distribution of bulk conductivity and the TDS, and specific conductance of groundwater in an aquifer contaminated with hydrocarbons and undergoing intrinsic biodegradation. Our objectives were to: (1) compare and validate TDS calculated from specific conductance using TDS determined by the gravimetric method for contaminated vs. uncontaminated locations, (2) determine whether TDS at contaminated locations are higher compared to uncontaminated locations as predicted by the Sauck (2000) conductive layer model, and (3) evaluate the relation-

ship between the bulk and fluid conductivity for sediments with variable hydrocarbon contamination and background (i.e. spatial variability).

2. Study site

The field site is near a former refinery (Crystal Refinery) located in Carson City, MI, USA (Fig. 1). Detailed descriptions of the study site can be found in Atekwana et al. (2000, 2004). Petroleum hydrocarbon releases (mostly JP4 jet fuel and diesel) from storage facilities and pipelines initially impacted sediments and groundwater more than 50 years ago. The contaminated aquifer has variable thickness (approximately 4.6 to 6.1 m thick) and composed of unconsolidated glacially derived sediments. Fine- to medium-grained sands characterize the unsaturated zone while the saturated zone consists of medium-sized sands and gravels underlain by a clay unit. The

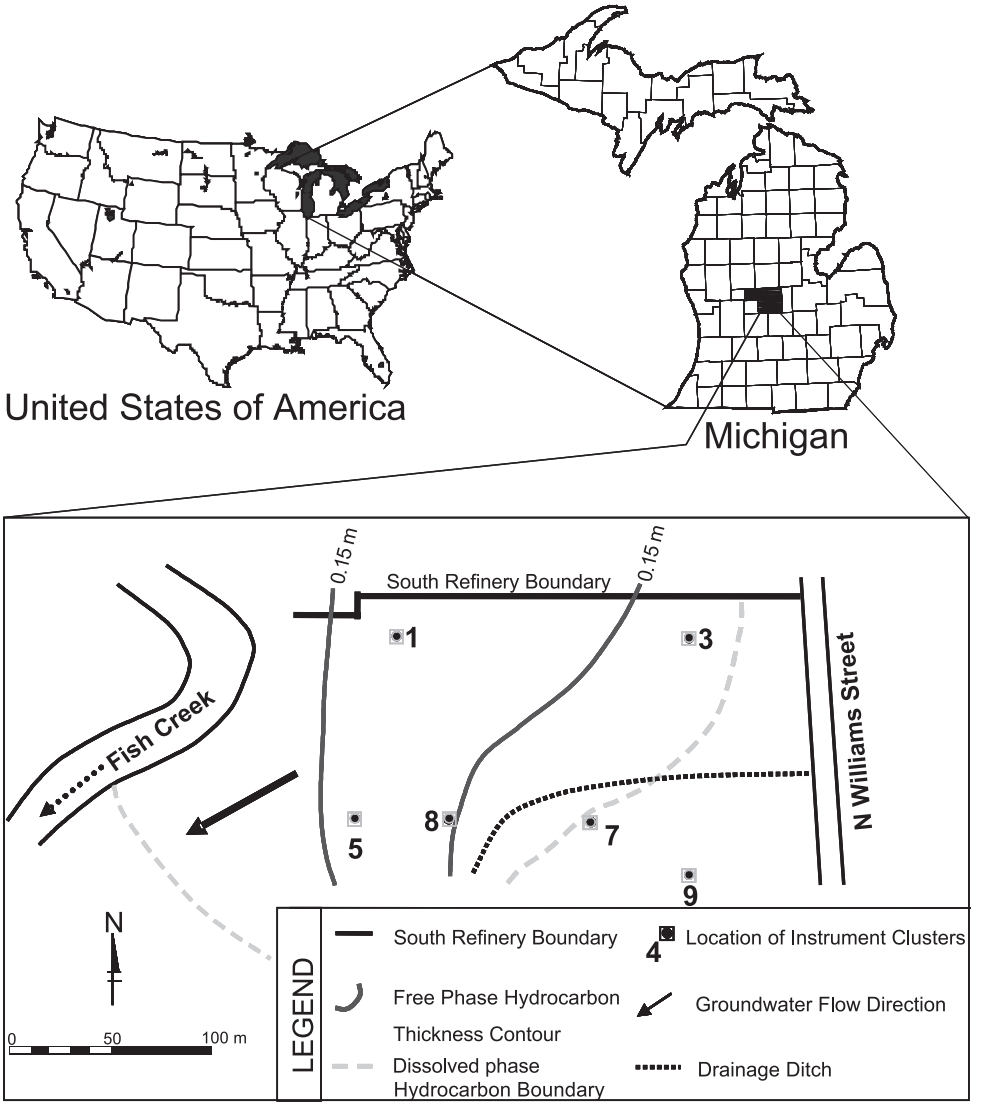

Fig. 1. Map of the study area showing hydrocarbon distribution in the groundwater. Also shown are locations where resistivity measurements were made and groundwater was sampled.

topography at the site is undulating causing the depths to the water table from the ground surface to vary between 0.6 and 0.9 m in the western portion and 4.6 and 5.8 m in the eastern portion of the study area. The groundwater table varies up to 0.9 m annually at the site (Werkema, 2002).

Hydrocarbon distribution at the study site is shown in Fig. 1. The hydrocarbon-contaminated locations are distinguished as the "plume core" and "plume fringe" based on the phase of hydrocarbon impacting the groundwater. Hydrocarbons trapped within the sediment pores (residual phase) and free flowing within the sediments (free phase) is the source of the dissolved hydrocarbon (dissolved phase) in groundwater that characterizes the core of the plume. Residual hydrocarbon is the contamination source of dissolved phase hydrocarbon at locations within the fringes of the plume (Dell Engineering, 1992; Legall, 2002).

Previous geoelectrical measurements at this study site have documented higher bulk conductivity in subsurface regions impacted by hydrocarbons compared to uncontaminated locations (Atekwana et al., 2004). The highest bulk conductivities were found to be associated with zones straddling the water table at locations in the plume core and fringe (Werkema et al., 2003; Atekwana et al., 2004). Intrinsic biodegradation is documented in the contaminated groundwater at the site. Methanogenesis is the dominant redox process within the core of the plume, while sulfate, iron, and manganese reduction occur at the fringes of the plume (Legall, 2002). Volatile organic acids and biosurfactants have been measured in contaminated groundwater at this site (Cassidy et al., 2002). Microbial studies in soil cores and groundwater in the contaminated aquifer have documented microorganisms capable of degrading hydrocarbon and show orders of magnitude higher oil degrading microorganisms within the hydrocarbon impacted zones (Duris et al., 2000; Cassidy et al., 2002; Atekwana et al., 2004).

3. Methods

The study site has been instrumented at several locations (Fig. 1). Each instrument location has a vertical resistivity probe (VRP) for making the resistivity measurements (converted to conductivity in this paper) and multilevel piezometers (MLPs; located approximately 1.0 m from the VRPs) for sampling groundwater. Details of the installation of the VRPs are described elsewhere by Werkema (2002). The MLPs were constructed of 6.4 mm PVC tubing fitted with a 15 cm nylon screen and were installed using a Geoprobe drill rig (Legall, 2002). The piezometers were installed at intervals of 30 cm from the base of the aquifer into the vadose zone. The locations where measurements were measured for this study are shown in Fig. 1. These include three locations in the core of the plume (Instrument clusters 1, 5 and 8), one location at the fringe of the plume (Instrument cluster 3), another location at or near the plume boundary (Instrument cluster 7), which was uncontaminated at the time of this study, and a location uncontaminated with hydrocarbon (Instrument cluster 9). Bulk conductivity measurements and groundwater analyses for specific conductance and TDS were conducted in June 2000.

3.1. Bulk electrical conductivity measurements

In situ bulk conductivity measurements were made from the VRPs using a 5 cm Wenner array and incremented every 5 cm with depth below ground surface. Details of these measurements are described elsewhere by Atekwana et al. (2004) and Werkema (2002). To relate the geophysical data to the groundwater data, only the bulk conductivity measurements below the water table are presented.

3.2. Groundwater specific conductance and TDS measurements

Groundwater specific conductance and TDS were measured with a conductivity/TDS meter in the field, while the gravimetric TDS was determined in the laboratory. In the field, groundwater from each multilevel piezometer was pumped to the surface using a peristaltic pump. The water was passed through a flow cell into which a HydroLab™ downhole Minisonde was immersed. Groundwater from piezometers was purged while the temperature, pH, and specific conductance were monitored until they stabilized. After stabilization of these parameters, the specific conductance and TDS were recorded. The

TDS values displayed by the conductivity/TDS meter is calculated from the specific conductance of groundwater and can be approximated by the following equation (e.g., Lloyd and Heathcote (1985):

$$TDS = k_e EC \quad (1)$$

where TDS is expressed in milligram per liter and EC is the electrical conductivity in microsiemens per centimeter at 25 °C (specific conductance). The correlation factor k_e varies between 0.55 and 0.8. The k_e for samples measured using the conductivity/TDS meter in this study was 0.64 regressed from the TDS vs. specific conductance data.

Groundwater sampled for gravimetric determination of TDS was collected immediately after TDS was measured by the HydroLab™ downhole Minisonde. Samples were collected in 250-ml polyethylene containers, stored on ice, transported to the laboratory and refrigerated at 4 °C until analyses, which were completed within 4 weeks of sample collection. Gravimetric TDS is defined as the weight of the residue (mg) in a known volume of water sample (l) after evaporating all the water. Dissolved solids by convention are defined as all solid material which is less than 0.45 μm in size. TDS was measured using Standard Methods 2540 C (Clesceri et al., 1989). A 100 ml of a well-mixed sample was filtered through a 0.45 μm glass fiber filter and washed with three successive aliquots of 10 ml deionized water. Complete drainage was allowed between washings, and suction continued for about 3 min after filtration was complete. The filtrate was transferred into a preweighed 200-ml beaker and evaporated to dryness in an oven for 24 h at 105 °C. The residue was then dried at 180 °C for exactly 2 h, cooled in a desiccator, and immediately weighed. The TDS for each sample was determined as the mass of solid normalized to the volume of water filtered.

3.3. TDS measurement of standard electrolyte solution

Natural waters contain a variety of both ionic and uncharged species in various amounts and proportions that constitute the dissolved solids. Thus it is not clear whether specific conductance measurements can be used to obtain accurate estimates of TDS. In addition, the effect of dissolved diesel on TDS measured by both the gravimetric and conductivity/TDS meter techniques needed to be determined using standard electrolyte solutions. The measured effect of dissolved hydrocarbon from standard electrolyte solutions should provide data to model our field data and to assess if discrepancies between TDS measured by both techniques were affected by dissolved hydrocarbon in groundwater.

Six NaCl standard solutions were prepared with specific conductance ranging between 5 and 150 mS/m for calibration of our field data. A 500-ml aliquot from each solution was transferred to a polyethylene container and 100 ml of diesel added to each solution. The containers of the NaCl+diesel solutions were placed on a shaker and shaken for 48 h to allow for maximum dissolution of diesel. This solution was kept undisturbed for 2 h to allow undissolved diesel to separate from the solution. The NaCl solution with dissolved phase diesel was used for the TDS experiments. TDS for the NaCl and NaCl+diesel solutions were measured using the conductivity/TDS meter. TDS was also measured using the gravimetric technique as described for the field samples.

4. Results and discussion

4.1. Relation of TDS values from specific conductance and gravimetric measurements to bulk conductivity of sediments

The results of TDS determined by the conductivity/TDS meter and gravimetric methods are presented in Table 1. Also shown in Table 1 are the bulk conductivity data (reported as the averaged bulk conductivity in mS/m over the interval where groundwater was sampled). TDS in uncontaminated groundwater (MLP9 and MLP7) measured using the conductivity/TDS meter ranged from 50 to 560 mg/l and 65 to 550 mg/l for the gravimetric technique. TDS in contaminated groundwater ranged from 123 to 681 mg/l and 150 to 810 mg/l for the conductivity/TDS meter and gravimetric techniques, respectively.

Vertical profiles of bulk conductivity and TDS determined by the conductivity/TDS meter and gravimetric techniques for uncontaminated locations are shown in Fig. 2a and b. Fig. 2 also shows sediment grain size distribution (% silt+clay, sand and gravel) for selected depth intervals which will be

Table 1
Sampling station, groundwater sampling depth, groundwater total dissolved solids, groundwater specific conductance and bulk electrical conductivity measured in uncontaminated and hydrocarbon contaminated locations in a shallow sandy aquifer

Sampling station[a]	Sampling depth (cm)[b]	TDS conductivity meter (mg/l)	TDS gravimetric (mg/l)	Specific conductance (mS/m)	Bulk electrical conductivity (mS/m)[c]	
MLP1						
MLP1-1	410	520	550	81.5	23.8	±6.6
MLP1-2	455	586	550	91.6	36.8	±6.9
MLP1-3	500	608	540	94.4	30.1	±3.0
MLP1-4	546	609	540	94.6	33.6	±2.0
MLP1-5	591	603	540	94.3	29.9	±0.9
MLP1-6	636	613	560	95.7	27.2	±2.4
MLP1-7	681	599	540	93.5	27.0	±1.4
MLP1-8	729	632	560	99.7	29.2	±2.1
MLP3						
MLP3-1	465	164	310	25.6	11.1	±2.2
MLP3-2	510	607	750	94.8	23.6	±4.1
MLP3-3	555	681	810	106.4	25.2	±1.9
MLP3-4	601	659	690	103.0	22.5	±1.9
MLP3-5	646	590	560	92.0	20.8	±1.2
MLP3-6	693	582	680	91.0	22.0	±1.2
MLP5						
MLP5-1	234	123	150	19.5	15.4	±5.5
MLP5-2	279	500	420	78.7	25.8	±4.5
MLP5-3	324	594	510	93.1	18.0	±3.7
MLP5-4	369	571	500	89.1	17.9	±2.9
MLP5-5	417	573	570	88.5	17.2	±3.3
MLP7						
MLP7-1	164	50	65	7.8	17.0	±1.0
MLP7-2	210	132	120	20.7	12.3	±0.2
MLP7-3	255	356	340	55.4	13.1	±0.4
MLP7-4	303	526	490	81.2	–	–
MLP8						
MLP8-1	198	368	290	57.7	8.6	±1.7
MLP8-2	243	585	530	94.1	16.9	±3.1
MLP8-3	288	625	620	97.8	18.6	±1.9
MLP8-4	333	639	610	99.7	16.2	±1.4
MLP8-5	378	629	620	98.6	18.5	±0.9
MLP9						
MLP9-1	235	301	300	47.1	6.5	±1.0
MLP9-2	281	494	480	75.6	17.9	±0.4
MLP9-3	327	545	530	85.4	19.8	±0.2
MLP9-4	358	560	550	87.7	–	–

[a] MLPs designated with a "-1" are at the water table and higher numbers increase with depth below the water table.
[b] Sampling depth represents the middle of the piezometer screened interval of 15 cm.
[c] Bulk electrical conductivity is reported as the mean and standard deviation for the corresponding interval where groundwater was sampled for TDS and specific conductance measurements.

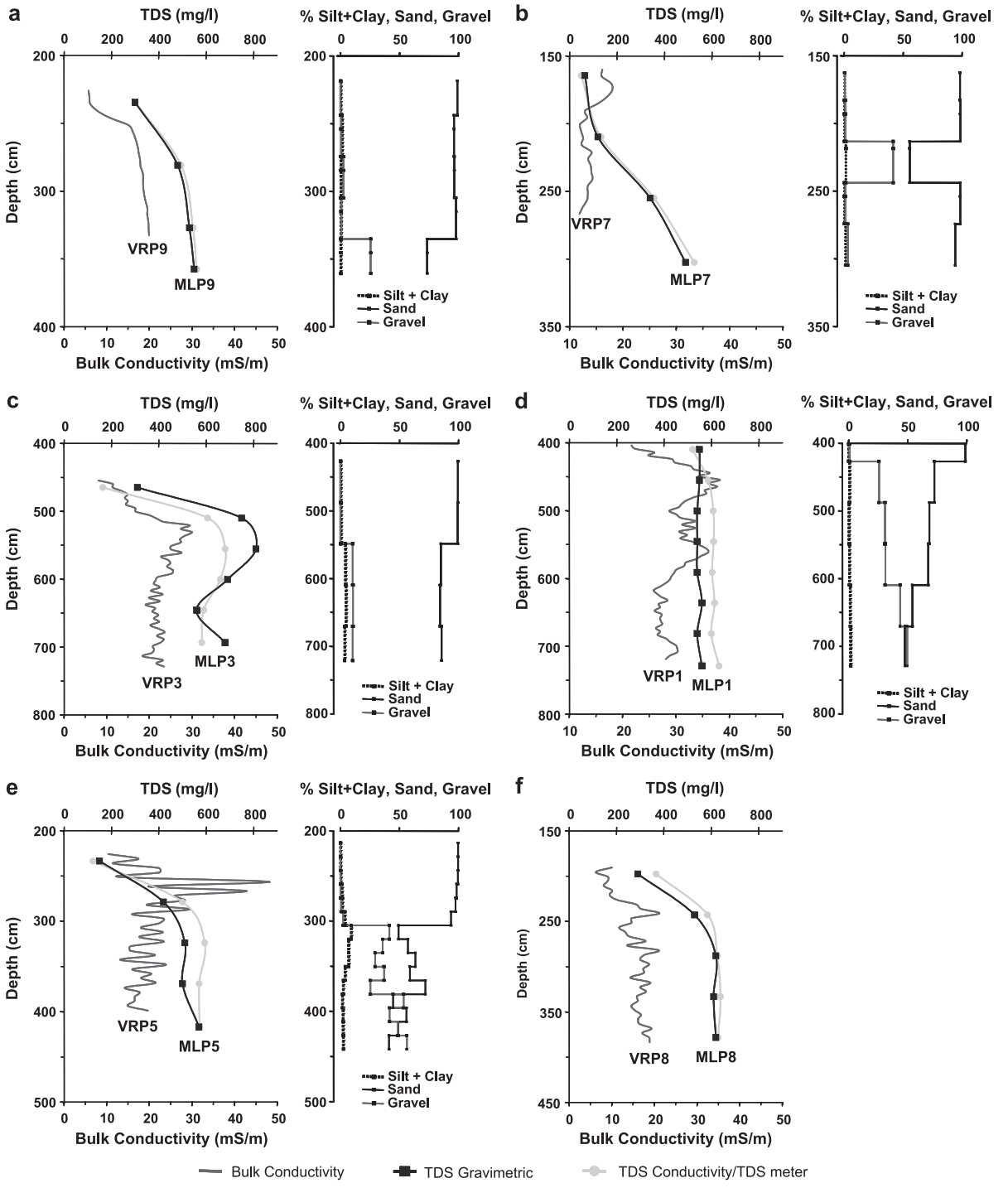

Fig. 2. Vertical profiles of sediment grain size distribution, bulk electrical conductivity of sediments, and total dissolved solids (TDS) Line 332 in groundwater from uncontaminated locations and locations contaminated with hydrocarbon. TDS values obtained from both gravimetric analysis and a conductivity/TDS meter are shown.

discussed later in Section 4.3. The bulk conductivity at VRP9 increases rapidly with depth (to 25 cm) below the water table, then increases slightly with depth to the base of the aquifer (Fig. 2a). The bulk conductivity at VRP7 increases with depth to about 15 cm below the water table before decreasing and remaining nearly constant to the base of the aquifer (Fig. 2b). The bulk conductivity values from the uncontaminated locations show maximum values of about 20 mS/m close to the bottom of the aquifer at VRP9 and the top of the aquifer at VRP7. TDS from both methods at MLP9 and MLP7 increased monotonically with depth. At these locations, the TDS measured using both methods were similar (averaged difference <15 mg/l). The bulk conductivity profile for VRP9 shows a similar depth trend to the TDS profile (Fig. 2a). This was not the case for MLP7, as the bulk conductivity was higher near the water table and decreased with depth (Fig. 2b).

In groundwater from the plume fringe at MLP3, TDS showed a steep positive gradient immediately below the water table, with peak values (30 mS/m) in mid aquifer, followed by a negative gradient (Fig. 2c). For most sampling depths at MLP3, TDS determined by the gravimetric technique was higher than TDS determined using the conductivity/TDS meter (Table 1). In addition, groundwater from MLP3 showed the greatest difference (~150 mg/l) in TDS between the two techniques (Table 1).

At MLP1 in the plume core, the TDS was generally high (~500 to 600 mg/l) and values for both techniques diverge below the water table and thereafter, the curves remained nearly parallel down to the base of the aquifer (Fig. 2d). TDS determined by the gravimetric technique was lower compared to that determined by the conductivity/TDS meter. Unlike the nearly constant TDS with depth, vertical variability in the bulk conductivity is observed in the depth profile (Fig. 2d) with peak values (~40 mS/m) occurring 50–150 cm below the water table. TDS in groundwater at the plume core from MLP5 and MLP8 also show steep positive gradients immediately below the water table with values remaining nearly constant at greater depths. TDS for groundwater at MLP5 and MLP8 determined by both techniques increase to peak values ~60 cm (594 and 639 mg/l, respectively) below the water table and converged towards the base of the aquifer (Fig. 2e and f). TDS measured by the gravimetric technique was generally lower than that measured using the conductivity/TDS meter. Peak bulk conductivity ranged from 26 to 19 mS/m for VRP 5 and 8, respectively.

4.1.1. Effect of dissolved hydrocarbon on TDS

The distribution of bulk conductivity and groundwater TDS for the different locations at the study site suggests a vertically and laterally heterogeneous system. Thus, to address our first objective, we assess the relationship between TDS determined by the conductivity/TDS meter and the gravimetric technique for uncontaminated and contaminated groundwater (Fig. 3). We assume that both techniques are measuring the same quantity and should have a 1:1 correlation. Also shown in Fig. 3 is the TDS data from the NaCl (solid line) and NaCl+diesel (dot-dash line) solutions. TDS determined by both methods for the NaCl and NaCl+diesel solutions are positively correlated (R^2>0.99). The slope of the NaCl solution is close to 1 (0.97) suggesting that the TDS determined by both techniques give nearly similar values. The NaCl+diesel solution had a lower slope (0.92) compared to that of the NaCl solution. We attribute the lower slope to: (1) dissolved diesel which contributed to the measured sample volume, but was lost in evaporation in the gravimetric technique, (2) a slight reduction in the electrical conductivity of the solution by the diesel, or (3) a combination of both.

Uncontaminated groundwater (MLP9 and MLP7; open symbols) plots along the NaCl solution correlation line (Fig. 3). Hydrocarbon contaminated groundwater samples (except from MLP3) plot either along the NaCl (solid line) or in some instances along or slightly below the NaCl+diesel (dot-dash line) solution line (Fig. 3). The samples that plot along or slightly below the NaCl+diesel line are from locations within the plume core with free phase hydrocarbon at the water table. The slightly lower TDS measured by the gravimetric technique for these samples is consistent with a decrease in the gravimetric TDS due to the presence of variably altered hydrocarbon dissolved in the groundwater and/or reduction in the electrical conductivity by dissolved hydrocarbons. Fig. 3 also shows that groundwater from MLP3 plots above the NaCl line, suggesting higher gravimetric TDS for groundwater from this location. The higher gravimetric TDS at MLP3 may be the result of

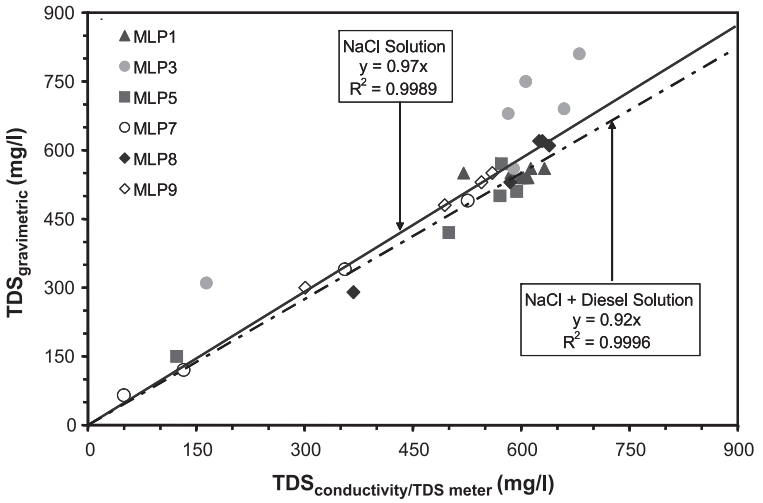

Fig. 3. Cross plot of total dissolved solids (TDS) measured by the conductivity/TDS meter and by the gravimetric method in groundwater from uncontaminated locations and locations contaminated with hydrocarbon. Contaminated groundwater samples are shown as filled symbols. Also shown are TDS values measured for a standard NaCl solution (solid line) and NaCl solution with dissolved diesel (dot-dashed line).

uncharged dissolved solids in the groundwater that did not contribute to the specific conductance measured by the conductivity/TDS meter.

4.2. Comparison of TDS at contaminated and uncontaminated locations

To address our second objective, we compare the TDS measured from contaminated and uncontaminated groundwater. We use TDS derived from the groundwater specific conductance to compare with the bulk conductivity, since this is the TDS routinely measured and reported for groundwater. The conductive layer model (Sauck, 2000) predicts higher TDS for groundwater in sediments contaminated with hydrocarbon and undergoing intrinsic biodegradation. Although there is overlap in the range of TDS values between uncontaminated and contaminated groundwater, TDS for contaminated groundwater samples are generally higher (up to 810 mg/l) compared to uncontaminated groundwater (up to 550 mg/l) (Table 1). The TDS results are consistent with findings from a geochemical study at this site, which showed higher calcium, silica, and bicarbonate ions in contaminated groundwater compared to uncontaminated groundwater (Legall, 2002). The Legall (2002) study also showed that the above ions accounted for more than 95% of the TDS in groundwater in this aquifer. Similar observations of higher levels of dissolved ions have been documented at other aquifers contaminated with hydrocarbon (e.g., McMahon et al., 1995). Further, in the McMahon et al. (1995) study, a positive correlation was observed between dissolved silica and organic acids. Thus, the higher TDS in contaminated groundwater is consistent with enhanced mineral weathering as predicted by the Sauck (2000) conductive layer model.

4.3. Relationship between bulk conductivity and fluid conductivity

To address our third objective, we examine the relationship between bulk and fluid conductivities from the study site. Archie (1942) proposed the following relationship which can be used to relate bulk and fluid conductivities in the absence of clays:

$$\sigma_b = a\phi^m S_w^n \sigma_w \quad (2)$$

where σ_b is the bulk electrical conductivity of the porous medium, a is a constant related to sediment type, ϕ is the porosity and m is the cementation factor, S_w is the water saturation and n is the saturation exponent and σ_w is the electrical conductivity of the pore fluids (fluid conductivity). Use of Eq. (2) assumes that the contribution of surface conduction

(conduction at the surfaces of mineral grains) compared with bulk conduction is negligible. However, when this is not the case, it has been shown from experimental work (Waxman and Smits, 1968; Sen et al., 1988) that Eq. (2) must be modified to include a surface conduction term (σ_s).

To explore the extent to which increase in TDS controls the bulk conductivity of contaminated sediments at this site, we make use of the relationship between the fluid conductivity (groundwater specific conductance in this study) and bulk conductivity in Fig. 4. We use the fluid conductivities instead of the TDS to keep the units of conductivity consistent with Eq. (2). Since, groundwater TDS is typically calculated from specific conductance, we expect the results to be essentially the same. Several observations can be made from the relationship between bulk and fluid conductivity (Fig. 4): (1) at low fluid conductivities less than 40 mS/m, the bulk conductivity is inversely related to the fluid conductivity. The samples that show this relationship occur at or near the water table. The low fluid conductivity for these samples probably result from the shorter time of interaction with the aquifer matrix (short residence time) and is consistent with new (spring) recharge to the aquifer. Note that except for MLP7, samples in this group are from contaminated locations. However, hydrocarbon has been detected in groundwater at MLP7 in the past (Dell Engineering, 1992), although none is currently present as the contaminant plume has shrunk over time. Groundwater at MLP7-1 (Table 1) had the lowest fluid conductivity but the highest bulk conductivity in this group. (2) Generally, at fluid conductivities greater than 40 mS/m, the bulk conductivity increased with increasing fluid conductivity, suggesting the dependence of bulk conductivity on fluid conductivity, consistent with Eq. (2) above. However, we also observed that at higher fluid conductivities (>80 mS/m) bulk conductivity increased without a corresponding increase in fluid conductivity, especially for contaminated groundwater samples (Fig. 4). The error bars of bulk conductivity for samples from contaminated locations (filled symbols) are larger than for uncontaminated samples (open symbols), consistent with steep vertical bulk conductivity gradients at the contaminated locations. (3) Fig. 4 also shows that samples with the highest bulk conductivity (MLP1) did not have the highest fluid conductivity.

We infer from the above observations that higher TDS in groundwater contributed to the higher bulk conductivity at locations contaminated with hydrocarbon consistent with the Sauck (2000) model. Nonetheless, the inverse relationship at low fluid conductivity and the poor positive relationship at high fluid conductivity especially for contaminated sam-

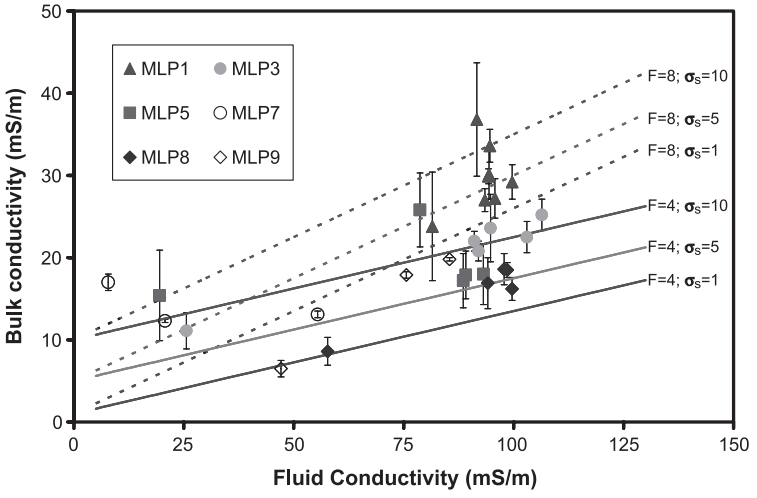

Fig. 4. Bulk electrical conductivity vs. fluid conductivity (groundwater specific conductance) from the study area. Groundwater samples contaminated with hydrocarbon are shown as filled symbols. Model lines are shown for selected formation factors (4–8) and surface conductivity (1–10 mS/m) calculated from Eq. (3) in the text.

ples suggest that the bulk conductivity at some locations was not entirely dependent on fluid conductivity, and that the bulk conductivity may be influenced by other factors.

Variations in saturation, lithology, and fluid conductivity are all factors that can affect bulk conductivity and may account for the variability in bulk conductivity vs. fluid conductivity observed at the site. We expect the effect of saturation to be minimal since all our data are from locations below the water table where sediments are fully saturated. The lithology at the study site is unconsolidated glacial outwash. Sediment grain size distribution data presented as percent gravel (>2 mm), sand (2–0.062 mm), and silt+clay (<0.062 mm) for selected depth intervals is shown (except VRP/MLP8) in Fig. 2. Depth intervals reported for the grain size distribution are either ~15 or 30 cm and were sampled at these intervals based on visual comparison using a Wards sediment Comparator (Wards Natural Science, Rochester, NY). The sediment distribution shows mainly sands near and above the water table, grading to a mixed sand and gravel below the water table (Fig. 2). A comparison of the dominant grain sizes with the vertical bulk conductivity from the VRPs shows little correspondence. For example, the change in bulk conductivity at VRP3 from the water table to ~60 cm below the water table occurs despite little change in sediment grain size in that interval (Fig. 2c). The above observation is common for contaminated locations and suggests that, although there are vertical variations in grain size at each location, lithology is not the dominant control of the bulk conductivity distribution. The highest increase in the silt+clay (up to 9%) content is measured for sediments from VRP5 between 310 and 375 cm, yet the bulk conductivity is lower within this interval than values measured for the interval between 250 and 300 cm where the lithology is dominated by sands (Fig. 2e). Although the actual clay content in the silt+clay was not determined, the bulk conductivity measured at VRP3 and the rest of the VRPs also show little correspondence between silt+clay and the bulk conductivity (Fig. 2). We assume from the above discussion that the effect of lithology on the bulk conductivity was minimal and is consistent with studies by Werkema et al. (2003).

We suggest two possible reasons for the inverse relationship at low fluid conductivity and poor positive relationship at higher fluid conductivity between the bulk and fluid conductivities at the site: (1) geochemical heterogeneity due to biological degradational processes not captured at the scale comparable to the bulk conductivity measurement. Water samples measured for TDS and fluid conductivity are integrated groundwater over the screened interval of 15 cm. On the other hand, the bulk conductivity was measured at a much finer resolution (5 cm). Because microbial degradation of hydrocarbon is vertically heterogeneous for each location (Legall, 2002), it is conceivable that the changes in the fluid conductivity resulting from this process occurs at the sub-centimeter scale not resolved by the groundwater sampling at 15-cm interval, but evident in the bulk conductivity measurement due to the higher resolution of the geophysical data. (2) Variations in interface conductivity. The Sauck (2000) model assumes mostly electrolytic conduction and does not take into account contributions from surface conductivity to measured bulk conductivity.

The direct current (dc) resistivity method as employed in this study is responsive to both electrolytic and interface (surface) conductivity. However, the bulk conductivity measured during this study, while diagnostic, does not differentiate between the relative contributions of electrolytic vs. interface conductivity. To assess the effects of surface conductivity on the measured bulk conductivity, we model the field data for formation factors in the range from 4 to 8 (typical for our site), and for surface conductivities from 1 to 10 mS/m (which covers our data range) using Eq. (3) over the whole range of fluid conductivity of our samples and assuming a water saturation of 1:

$$\sigma_b = \sigma_{el} + \sigma_s = 1/F(\sigma_w) + \sigma_s \quad (3)$$

where σ_{el} is electrolytic conductivity, σ_w is the fluid conductivity, σ_s is the surface conductivity, and F is the sample formation factor (Waxman and Smits, 1968). Model curves for different formation factors and surface conductivity are presented in Fig. 4 and suggest that no single F value or σ_s can fit our data; rather different combinations of σ_s and F are needed to explain the bulk conductivity–fluid conductivity distribution seen in the field data. For a given σ_s value, variation in F values from 4 to 8 over the range of fluid conductivity for field samples was not able to

explain the bulk conductivity–fluid conductivity distribution. A broad range in σ_s conductivity (1 to 10 mS/m) or F is needed to explain the relationships for the field samples. The model results further suggest that relative to F, σ_s has a greater influence on the bulk conductivity, especially from sediments currently or previously contaminated by hydrocarbon.

An investigation of sediments at the study site using induced polarization (IP) methods showed that contaminated samples had a higher imaginary conductivity (σ'') magnitude compared to uncontaminated samples (Abdel Aal et al., 2003). σ'' is the polarization term and at low frequencies (less than 1000 Hz) is an interfacial phenomenon occurring at the grain-fluid boundary surface in saturated porous media (e.g., Olhoeft, 1985; Schön, 1996). Hence, Abdel Aal et al. (2003) suggested that alteration of the mineral surface chemistry due to microbial activity may explain the higher magnitude in the IP response observed for contaminated sediments. This explanation is consistent with results from recent laboratory experiments that showed temporal increase in the real, imaginary, and surface conductivity during microbial degradation of diesel-contaminated sediments (Abdel Aal et al., 2004). We conclude that both electrolytic and surface conduction are factors that can account for the higher bulk conductivities observed in sediments impacted by hydrocarbon and undergoing biodegradation even in the absence of lithology dominated by clays.

5. Conclusions

The results of this study show that TDS and bulk conductivities of sediments are generally higher at locations contaminated with hydrocarbon and undergoing intrinsic biodegradation compared to uncontaminated locations. This observation is consistent with the conductive layer model of Sauck (2000). However, data from some contaminated locations showed an inverse relationship between bulk and fluid conductivity at low (<40 mS/m) fluid conductivity and a poor positive relationship between bulk and fluid conductivity for higher (>40 mS/m) fluid conductivity. We infer from our results that the bulk conductivity measured at the contaminated locations was affected by factors other than higher TDS. We note that electrolytic conduction assumed by the Sauck (2000) model and used in this study to control the formation bulk conductivity may be overly simplified. We conclude that electrolytic conduction may not be the only path of electrical conduction in hydrocarbon contaminated soils. Surface conductivity can occur along surfaces of mineral grains. While this study was conducted on the premise that electrical current flow in the aquifer was mainly electrolytic, hydrocarbon degradation and subsequent mineral weathering will not only increase the fluid conductivity but also alter the mineral surface properties resulting in an enhancement of the surface conduction at the mineral–fluid interface. This process may provide an additional path for electrical conduction not accounted for by pore fluid conductivity.

On a final note, Börner et al. (1993) suggest that the degree of the change in electrical properties of contaminated porous rocks is determined by the initial rock composition and structure, chemical and physical properties of the contaminating substances, concentration of the contaminants in the pore fluid, duration of interaction between rock and contaminant, and environmental thermodynamic factors such as temperature and pressure. We add to this list of factors, the influence of biogeochemical processes on the rock matrix. We suggest that at the present stage of the research, the question as to how the effects of microbial degradation of hydrocarbon, the degradation products, secondary mineral reactions in the aquifer matrix and groundwater influence the electrical properties is still open both to debate and further research.

Acknowledgements

This work was funded in part by the American Chemical Society-Petroleum Research Fund Grant (PRF # 31594-AC2). Ruth Rivera of Test America, Indianapolis, IN provided laboratory space and materials for gravimetric TDS analysis. The U.S. Environmental Protection Agency through its Office of Research and Development collaborated in this research. It has been subjected to the Agency's review and approved for publication. Mention of trade names or commercial products does not constitute an endorsement or recommendation for use. Comments

and suggestions from two anonymous reviewers helped improve this manuscript.

References

Abdel Aal, G.Z., Atekwana, E.A., Slater, L.D., Ulrich, C., 2003. Induced polarization (IP) measurements of soils from an aged hydrocarbon contaminated site. Proceedings of the Symposium on the Application of Geophysics to Engineering and Environmental Problems, San Antonio, Texas, April 6–10, pp. 190–202.

Abdel Aal, G.Z., Atekwana, E.A., Slater, L.D., Atekwana, E.A., 2004. Effects of microbial processes on electrolytic and interfacial electrical properties of unconsolidated sediments. Geophys. Res. Lett. 31 (12), L12505.

Archie, G.E., 1942. The electrical resistivity log as an aid in determining some reservoir characteristics. Trans. Am. Inst. Min. Metall. Pet. Eng. 146, 54–62.

Atekwana, E.A., Sauck, W.A., Werkema, D.D., 2000. Investigations of geoelectrical signatures at a hydrocarbon contaminated site. J. Appl. Geophys. 44, 167–180.

Atekwana, E.A., Sauck, W.A., Abdel Aal, G.Z., Werkema, D.D., 2002. Geophysical investigation of vadose zone conductivity anomalies at a hydrocarbon contaminated site: implications for the assessment of intrinsic bioremediation. J. Environ. Eng. Geophys. 7, 103–110.

Atekwana, E.A., Werkema, D.D., Duris, J.W., Rossbach, S., Atekwana, E.A., Sauck, W.A., Cassidy, D.P., Means, J., Legall, F.D., 2004. In-situ apparent conductivity measurements and microbial population distribution at a hydrocarbon contaminated site. Geophysics 69, 56–63.

Börner, F., Gruhne, M., Schön, J., 1993. Contamination indications derived from electrical properties in the low frequency range. Geophys. Prospect. 41, 83–98.

Cassidy, D.P., Werkema, D.D., Sauck, W.A., Atekwana, E.A., Rossbach, S., Duris, J., 2001. The effects of LNAPL biodegradation products on electrical conductivity measurements. J. Environ. Eng. Geophys. 6, 47–52.

Cassidy, D.P., Hudak, A.J., Werkema, D.D., Atekwana, E.A., Rossbach, S., Duris, J.W., Atekwana, E.A., Sauck, W.A., 2002. In-situ Rhamnolipid production at an abandoned petroleum refinery by *Pseudomonas aeruginosa*. J. Soil Sed. Contam. 11, 769–787.

Clesceri, L.S., Greenberg, A.E., Trussell, R.R., 1989. Standard Methods for the Examination of Water and Wastewater. American Public Health Association, Washington, DC.

Cozzarelli, I.M., Eganhouse, R.P., Baedecker, M.J., 1990. Transformation of monoaromatic hydrocarbons to organic acids in anoxic groundwater environment. Environ. Geol. Water Sci. 16, 135–141.

Cozzarelli, I.M., Baedecker, M.J., Eganhouse, R.P., Goerlitz, D.F., 1994. The geochemical evolution of low-molecular-weight organic acids derived from the degradation of petroleum contaminants in groundwater. Geochim. Cosmochim. Acta 58, 863–877.

Cozzarelli, I.M., Bekins, B.A., Baedecker, M.J., Aiken, G.R., Eganhouse, R.P., Tuccillo, M.E., 2001. Progression of natural attenuation processes at a crude oil spill site: I. Geochemical evolution of the plume. J. Cont. Hydrogeology 53, 369–385.

De Ryck, S.M., Redman, J.D., Annan, A.P., 1993. Geophysical monitoring of a controlled kerosene spill. Proceedings of the Symposium on the Application of Geophysics to Engineering and Environmental Problems, San Diego, CA, pp. 5–19.

Dell Engineering, 1992. Remedial Action Plan for Crystal Refining Company, 801 North Williams Street, Carson City, MI. Report DEI No. 921660, Holland, MI.

Duris, J.W., Werkema, D.D., Atekwana, E.A., Eversole, R., Beuving, L., Rossbach, S., 2000. Microbial communities and their effects on silica structure and geophysical properties in hydrocarbon impacted sediments. Program Abstr.-Geol. Assoc. Can. 32, A-190.

Hem, J.D., 1985. Study and Interpretation of the Chemical Characteristics of Natural Water, 3rd ed. U.S. Geological Survey Water-Supply Paper, vol. 2254. Washington, DC.

Legall, F.D., 2002. Geochemical and isotopic characteristics associated with high conductivities in a shallow hydrocarbon contaminated aquifer. Unpublished PhD dissertation, Western Michigan University, 85 pp.

Lloyd, J.W., Heathcote, J.A., 1985. Natural Inorganic Hydrochemistry in Relation to Groundwater. Clarendon Press, Oxford, England.

Mazác, O., Benes, L., Landa, I., Maskova, A., 1990. In: Ward, S.H. (Ed.), Determination of the Extent of Oil Contamination in Groundwater by Geoelectrical Methods, Geotech. Environ. Geophys., vol. II, pp. 107–112.

McMahon, P.B., Vroblesky, D.A., Bradely, P.M., Chapelle, F.H., Gullet, C.D., 1995. Evidence for enhanced mineral dissolution in organic acid-rich shallow ground water. Ground Water 33, 207–216.

Olhoeft, G.R., 1985. Low frequency electrical properties. Geophysics 50, 2492–2503.

Sauck, W.A., 2000. A conceptual model for the geoelectrical response of LNAPL plumes in granular sediments. J. Appl. Geophys. 44, 151–165.

Sauck, W.A., Atekwana, E.A., Nash, M.S., 1998. Elevated conductivities associated with an LNAPL plume imaged by integrated geophysical techniques. J. Environ. Eng. Geophys. 2–3, 203–212.

Schneider, G.W., Greenhouse, J.P., 1992. Geophysical detection of perchloroethylene in a sandy aquifer using resistivity and nuclear logging techniques. Proceedings of the Symposium on the Application of Geophysics to Engineering and Environmental Problems, Oakbrook, IL, pp. 619–628.

Schön, J.H., 1996. Physical Properties of Rocks—Fundamentals and Principles of Petrophysics, Handbook of Geophysical Exploration, Seismic Exploration, vol. 18. Pergamon, Oxford, UK. 583 pp.

Sen, P.N., Goode, P.A., Sibbit, A., 1988. Electrical conduction in clay bearing sandstones at low and high salinities. J. Appl. Phys. 63, 4832–4840.

Shevnin, V., Mousatov, A., Nakamura-Labastida, E., Delgado-Rodriquez, O., Mejia-Aguilar, A., Sanchez-Osi, J., Sanchez-

Osio, H., 2003. Study of pollution in airports with resistivity sounding. Proceedings of the Symposium on the Application of Geophysics to Engineering and Environmental Problems, San Antonio, TX, pp. 180–189.

Waxman, M.H., Smits, L.J.M., 1968. Electrical conductivities in oil-bearing shaley sands. Soc. Pet. Eng. 8, 107–122.

Werkema, D.D., 2002. Geoelectrical response of an aged LNAPL plume: implications for monitoring natural attenuation. Unpublished PhD dissertation, Western Michigan University, 136 pp.

Werkema, D.D., Atekwana, E.A., Endres, A., Sauck, W.A., Cassidy, D.P., 2003. Investigating the geoelectrical response of hydrocarbon contamination undergoing biodegradation. Geophys. Res. Lett. 30, 1647.

Wood, W.W., 1976. Guidelines for collection and field analyses of groundwater samples for selected unstable constituents. Techniques of Water-Resources Investigations of the United States Geological Survey, Book 1, Chapter D2. U.S. Geological Survey, Washington, DC.